Convergence Analysis of the Rebalance Methods of Discrete Ordinates Transport Equation For Eigenvalue Problems

Ser Gi Hong, Kang-Seog Kim, and Jae-Seung Song
Korea Atomic Energy Research Institute, Duckjin-dong, Yuseong-gu, Daejon
hongsg@kaeri.re.kr

1. Introduction

This paper analyzes the convergence of the rebalance methods[1,2] (e.g., Coarse-Mesh Rebalance (CMR), Coarse-Mesh Finite Difference (CMFD), and *p*-CMFD) for accelerating the power iteration method of the discrete ordinates transport equation in the eigenvalue problem[3]. The convergence analysis is done with the well-known Fourier analysis method through a linearization both for spatially continuous and discretized forms of one and two energy group transport equations in an infinite medium.

2. Theory and Methodology

Although the analysis was performed both for the spatially continuous and discretized cases of the one and two-group problems, the description of the analysis is given only for the spatially continuous forms of the discrete ordinates transport equations and the rebalance equation for the two-group eigenvalue problem for simplicity. They are given by

$$\mu_m \frac{\partial \psi_{1,m}^{l+1/2}}{\partial x} + \sigma_1 \psi_{1,m}^{l+/2} = \sigma_{s1}\phi_1^l + \sigma_{2\to 1}\phi_2^l + \frac{1}{k_{eff}^l}(\nu\sigma_{f1}\phi_1^l + \nu\sigma_{f2}\phi_2^l), \quad (1a)$$

$$\mu_m \frac{\partial \psi_{2,m}^{l+1/2}}{\partial x} + \sigma_2 \psi_{2,m}^{l+/2} = \sigma_{s2}\phi_2^l + \sigma_{1\to 2}\phi_1^{l+1/2},$$

$$\phi_1^{l+1/2} = \sum_{m=1}^{M} w_m \psi_{1,m}^{l+1/2}, \phi_2^{l+1/2} = \sum_{m=1}^{M} w_m \psi_{2,m}^{l+1/2},$$

and

$$D_g^{\pm,l} = \frac{2J_g^{\pm} \pm D_g \frac{\partial \phi_g^{l+1/2}}{\partial x}}{2\phi_g^{l+1/2}}, \quad (1b)$$

$$-D_1 \frac{\partial^2 \phi_1^l}{\partial x^2} + D_1^{+,l} \frac{\partial \phi_1^{l+1}}{\partial x} - D_1^{-,l} \frac{\partial \phi_1^{l+1}}{\partial x} + \sigma_1 \phi_1^{l+1} = \sigma_{s1}\phi_1^{l+1} + \sigma_{2\to 1}\phi_2^{l+1}$$

$$+ \frac{1}{k_{eff}^{l+1}}(\nu\sigma_{f1}\phi_1^{l+1} + \nu\sigma_{f2}\phi_2^{l+1}),$$

$$-D_2 \frac{\partial^2 \phi_2^l}{\partial x^2} + D_2^{+,l} \frac{\partial \phi_2^{l+1}}{\partial x} - D_2^{-,l} \frac{\partial \phi_2^{l+1}}{\partial x} + \sigma_2 \phi_2^{l+1} = \sigma_{s2}\phi_2^{l+1} + \sigma_{1\to 2}\phi_1^{l+1}.$$

In Eq.(1), l is the outer iteration index, one inner iteration (i.e., one transport sweeping) for each outer iteration is assumed, and $D^{\pm}$ represents the correction factor for preserving the partial currents in the rebalance equation. It should be noted in Eq.(1b) that there is no equation for updating the multiplication factor. These equations are linearized around the fluxes and the multiplication factor of the infinite medium. The resulting linearized equations are given by

$$\mu_m \frac{\partial \xi_{1,m}^{l+1/2}}{\partial x} + \sigma_1 \xi_{1,m}^{l+/2} = [\sigma_{s1} + \frac{\nu\sigma_{f1}}{k_\infty}]\varsigma_1^l + [\frac{\sigma_{1\to 2}\nu\sigma_{f2}}{\sigma_{R2}k_\infty} + \frac{\sigma_{2\to 1}\sigma_{1\to 2}}{\sigma_{R2}}]\varsigma_2^l \quad (2a)$$

$$+ [\frac{\nu\sigma_{f1}}{k_\infty} + \frac{\sigma_{1\to 2}\nu\sigma_{f2}}{\sigma_{R2}k_\infty}]\delta^l,$$

$$\mu_m \frac{\partial \xi_{2,m}^{l+1/2}}{\partial x} + \sigma_2 \xi_{2,m}^{l+/2} = \sigma_{s2}\varsigma_2^l + \sigma_{R2}\varsigma_1^{l+1/2},$$

$$\varsigma_1^{l+1/2} = \sum_{m=1}^{M} w_m \xi_{1,m}^{l+1/2}, \varsigma_2^{l+1/2} = \sum_{m=1}^{M} w_m \xi_{2,m}^{l+1/2},$$

and

$$-D_1 \frac{\partial^2 \varsigma_1^{l+1}}{\partial x^2} + \sum_{m=1}^{M} w_m \mu_m \xi_{1,m}^{l+1/2} + D_1 \frac{\partial^2 \varsigma_1^{l+1/2}}{\partial x^2} + \sigma_1 \varsigma_1^{l+1} = [\sigma_{s1} + \frac{\nu\sigma_{f1}}{k_\infty}]\varsigma_1^{+1l} \quad (2b)$$

$$+ [\frac{\sigma_{1\to 2}\nu\sigma_{f2}}{\sigma_{R2}k_\infty} + \frac{\sigma_{2\to 1}\sigma_{1\to 2}}{\sigma_{R2}}]\varsigma_2^{l+1} + [\frac{\nu\sigma_{f1}}{k_\infty} + \frac{\sigma_{1\to 2}\nu\sigma_{f2}}{\sigma_{R2}k_\infty}]\delta^{l+1},$$

$$-D_2 \frac{\partial^2 \varsigma_2^{l+1}}{\partial x^2} + \sum_{m=1}^{M} w_m \mu_m \xi_{2,m}^{l+1/2} + D_2 \frac{\partial^2 \varsigma_2^{l+1/2}}{\partial x^2} + \sigma_2 \varsigma_2^{l+1} = \sigma_{s2}\varsigma_2^{l+1} + \sigma_{R2}\varsigma_1^{l+1}$$

In Eq.(2), σ_{Rg} is the removal cross section. ξ, ζ, and δ are the first-order terms in ε of the angular flux (ψ), scalar flux (ϕ), and $1/(k_{eff})$, respectively. To perform the Fourier analysis, the following ansatz are introduced :

$$\xi_{g,m}^{l+1/2} = \varpi^l A_{g,m} e^{j\lambda x}, \zeta_g^l = \varpi^l a_g e^{j\lambda x}, \delta^l = b\varpi_0^l \quad (3)$$

In this equation, ϖ is the eigenvalue of the power iteration and ϖ_0 is the eigenvalue for the fundamental mode. In Eq.(3), it is noted that the ansatz δ has no spatial dependency because the multiplication factor has no dependency on *x*. A simple algebra shows the fundamental eigenvlaue (ϖ_0) is zero. Substituting Eq.(3) into Eq.(2) gives the eigenvalue as a function of the frequency (λ) and the spectral radius is the largest eigenvalue in an absolute value. In this paper, we omitted the detailed expression of the spectral radius for simplicity. In fact, it is not difficult to show that the spectral radius of the power iteration can be obtained by using the one of the outer iteration for a fixed source problem but using the following transformation of the cross sections :

$$\sigma_{s1} + \frac{\nu\sigma_{f1}}{k_\infty} \Rightarrow \sigma_{s1}, \frac{\nu\sigma_{f2}\sigma_{1\to 2}}{k_\infty \sigma_{R2}} + \frac{\sigma_{2\to 1}\sigma_{1\to 2}}{\sigma_{R2}} \Rightarrow \sigma_{2\to 1}, \quad (4)$$

$$\sigma_{s2} \Rightarrow \sigma_{s2}, \sigma_{R2} \Rightarrow \sigma_{1\to 2}$$

3. Numerical Analysis and Discussion

For the numerical analysis, we chose a reference set of the cross sections. This reference set of the cross sections is given in Table 1. We used only p-CMFD, the step characteristic (SC) method, and S_{10} angular

quadrature set for the numerical test although our formulation is general.

Table 1: Reference set of the cross sections for the benchmark problem

Group 1	σ_1	σ_{s1}	$\sigma_{1\to2}$	$\nu\sigma_{f1}$
	0.3	0.27	0.01	0.008476
Group 2	σ_2	σ_{s2}	$\sigma_{2\to1}$	$\nu\sigma_{f2}$
	1.0	0.9	0.001	0.18514

We consider the following four cases : the first case (Case I) is the reference described above, 2) the second case(Case II) has the same cross sections as the reference case but it has increased self-group scattering cross sections ($\sigma_{s1} = \sigma_1 - \sigma_{1\to2} = 0.29$ and $\sigma_{s2} = \sigma_2 - \sigma_{2\to1} = 0.999$), and the third case (Case III) is the same as the reference case but it has different fission cross sections given by $\nu\sigma_{f1} = k_\infty(\sigma_1 - \sigma_{s1} - \sigma_{1\to2})$ and $\nu\sigma_{f2} = k_\infty(\sigma_2 - \sigma_{s2} - \sigma_{2\to1})$ in which k_∞ is the infinite multiplication factor of the reference case, and the fourth case (Case IV) is the same as the reference case but it has artificially large fission cross sections given by $\nu\sigma_{f1} = \nu\sigma_{f2} = 10.0$. Fig.1 compares the spectral radii versus mesh size for the fixed source and eigenvalue problems for the reference case. It is shown that the spectral radius of the eigenvalue problem is larger than that of the fixed source problem and their difference is larger in the large mesh size region than in the small mesh size region.

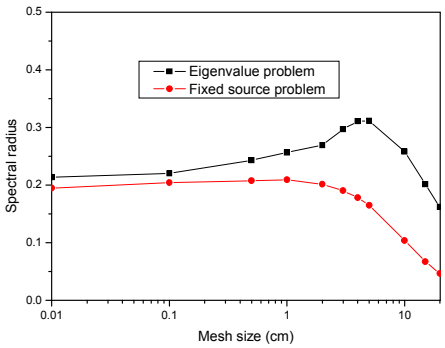

Fig. 1. Spectral radii versus mesh size (reference case)

Fig. 2 compares the spectral radii of the four cases for the eigenvalue problem. This figure shows that the spectral radius of the power iteration depends both on the fission cross sections and the scattering matrix but its dependency on the fission cross sections is not strong. For numerical test, a benchmark problem is devised. Its size is 1000cm and it has the cross sections of the reference case described above. The vacuum boundary conditions are imposed both on the left and right boundaries. The point-wise convergence criteria of 10^{-7} and 10^{-12} on the fission source are used for the transport and rebalance equations, respectively. In these calculations, we considered the four mesh sizes given in Table 2.

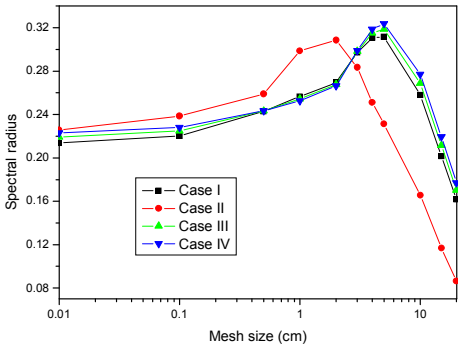

Fig. 2. Comparison of spectral radii versus mesh sizes

Table 2 compares the numerical spectral radii and the theoretical ones for this benchmark problem. As shown in Table 2, the theoretical predicted spectral radius has a good agreement with the numerically estimated spectral radius. Table 2 shows that the power iteration without the acceleration has very slow convergence (spectral radius ~1.0). In fact, it is possible to show that the power iteration without the acceleration has unity spectral radius irrespective of the cross sections and the mesh sizes for eigenvalue problem. As a conclusion, our analysis provides a theoretical base of the convergence of the power iteration for the discrete ordinates transport equation.

Table 2: Comparison of the numerical and theoretical spectral radii

Mesh size (cm)	Without p-CMFD			With p-CMFD		
	N	ρ^{th}	ρ^{nu}	N	ρ^{th}	ρ^{nu}
2.0	35463	1.0	0.9996	11	0.269	0.248
5.0	26432	1.0	0.9995	12	0.312	0.268
10.0	16853	1.0	0.9991	11	0.258	0.232
20.0	9537	1.0	0.9985	8	0.162	0.124

Acknowledgement

This work is supported by "Development of the Major Design Codes for a Nuclear Power Plant" Project sponsored by Korea Ministry of Commerce, Industry and Energy.

REFERENCES

[1] N. Z. Cho and G. S. Lee, "Comparison of CMFD and p-CMFD Acceleration Methods for Neutron Transport Calculations," *Proc. of Korean Nuclear Society*, Gyeongju, Korea, May 2003.

[2] G. R. Cefus and E. W. Larsen, "Stability Analysis of Coarse-Mesh Rebalance," *Nucl. Sci. Eng.*, **105**, 31(1990).

[3] H. C. Lee et al., "Fourier Convergence Analysis of Two-Dimensional/One-Dimensional Coupling Methods for the Three-Dimensional Neutron Diffusion Eigenvalue Problems," *Nucl. Sci. Eng.*, **156**, 74(2007).